# Prospects of non-resonant Higgs pair production at the HL-LHC and HE-LHC

# Prospects of non-resonant Higgs pair production at the HL-LHC and HE-LHC

**Amit Adhikary[1], Shankha Banerjee[2], Rahool Kumar Barman[3], Biplob Bhattacherjee[1] and Saurabh Niyogi[4]**

[1] Centre for High Energy Physics, Indian Institute of Science, Bangalore 560012, India
[2] Institute for Particle Physics Phenomenology, Department of Physics, Durham University, Durham DH1 3LE, United Kingdom
[3] School of Physical Sciences, Indian Association for the Cultivation of Science, Kolkata 700032, India
[4] Gokhale Memorial Girls' College, Kolkata, India

E-mail: amitadhikary@iisc.ac.in

**Abstract.** The prospects of observing the di-Higgs production in the Standard Model (SM) is explored. We choose final states based on considerable production rate and cleanliness. Standard cut-based and multivariate analyses using the Boosted Decision Tree (BDT) algorithm is performed at the high luminosity run of the 14 TeV LHC (HL-LHC) and we got a combined signal significance of $\sim 2.1$. For the proposed high energy upgrade of the LHC (HE-LHC) at $\sqrt{s}$ = 27 TeV, we do multivariate analyses using BDT algorithm, the XGBoost toolkit and Deep Neural Network (DNN), and we observe a discovery prospect with $> 5\sigma$ significance for the Higgs pair production.

## 1. Introduction

The Higgs boson which constitutes the scalar sector in the Standard Model (SM) has been observed at the Large Hadron Collider (LHC) by ATLAS [1] and CMS [2] collaboration in 2012. After that, properties of the Higgs boson are being measured with precision by collecting more data over the years, namely, its coupling to the various SM particles, its width, spin and $CP$ properties. Another important property related to Higgs physics is its self-coupling ($\lambda_{hhh}$) which determines the nature of the Higgs potential. The value of $\lambda_{hhh}$ in SM is fixed by the mass of the Higgs boson and vacuum expectation value of Higgs potential. However, a direct measurement of this coupling at experiment is crucial which is a challenging task. The main difficulty lies in the production rate of Higgs pair which proceeds through a top quark loop (triangle diagram) in dominant production mode via gluon fusion channel. Also a box diagram of top quark loop contribute to this di-Higgs production with destructive interference and thus reducing the overall production rate at the LHC. The Higgs pair production cross-section at $\sqrt{s} = 14$ TeV is $36.69^{+2.1\%}_{-4.9\%}$ fb [3] at NNLO level, while at $\sqrt{s} = 27$ TeV it becomes $139.9^{+1.3\%}_{-3.9\%}$ fb [3] at NNLO which is approximately 4 times larger than at $\sqrt{s} = 14$ TeV. To observe Higgs pair production at the experiment, we have to look for possible final states arising from decay of the two Higgs bosons.

We choose various di-Higgs final states based on production rate and cleanliness. First, we study di-Higgs production at the HL-LHC ($\sqrt{s} = 14$ TeV with 3 $ab^{-1}$ of integrated luminosity)

in the $b\bar{b}\gamma\gamma$, $b\bar{b}\tau\tau$, $b\bar{b}WW^*$, $WW^*\gamma\gamma$ and $4W$ final states [4]. Here, we do standard cut-based analysis along with multivariate analysis based on the Boosted Decision Tree (BDT) algorithm in the `TMVA` framework [5]. Next, we analyse the prospect of di-Higgs production at the HE-LHC ($\sqrt{s} = 27$ TeV with 15 $ab^{-1}$ of integrated luminosity) in the $b\bar{b}\gamma\gamma$, $b\bar{b}\tau\tau$, $b\bar{b}WW^*$, $WW^*\gamma\gamma$, $b\bar{b}ZZ^*$ and $b\bar{b}\mu\mu$ channels [6]. In order to improve over the signal significance, we adopt three different multivariate analysis techniques, namely, BDT algorithm, `XGBoost` toolkit [7] and Deep Neural Network (DNN) [8–10].

## 2. Higgs pair production at the HL-LHC

In this section, we present the details of the study on various final states coming from di-Higgs production at the centre of mass energy of $\sqrt{s} = 14$ TeV with 3 $ab^{-1}$ of integrated luminosity. To simulate the di-Higgs signal and background samples, we use `MG5_aMC@NLO` [11] with NN23LO parton distribution function (PDF) [12] and default factorisation and renormalisation scales. These events are showered and hadronised via `Pythia-6` [13]. We use anti-$kT$ [14] algorithm to reconstruct jets with $p_T > 20$ GeV and jet radius parameter of $R = 0.4$ in the `FastJet` [15] framework. Next, we simulate the detector effects using `Delphes-3.4.1` [16]. The isolation criteria for electrons, muons and photons are defined as the energy activity within a cone of $\Delta R = 0.5$ around these objects, is required to be $< 12\%, 25\%$ and $12\%$ of their transverse momentum, $p_T$ respectively. The $b$-tagging efficiency, $j \to b$ and $c \to b$ mistagging efficiency are taken to be 70%, 1% and 30% respectively. We consider a $j \to \gamma$ fake rate of $\sim 0.1\%$. Also, an electron or a muon is referred as a lepton ($\ell$) throughout the text unless mentioned separately.

### *2.1. The $b\bar{b}\gamma\gamma$ channel*

Here, we study di-Higgs production in the $b\bar{b}\gamma\gamma$ final state. This channel is clean in terms of photons in the final state but suffers from production rate because of tiny branching ratio of $h \to \gamma\gamma$. The dominant background contribution comes from the $b\bar{b}\gamma\gamma$ process. Also, we generate sub-dominant backgrounds like $t\bar{t}h$, $b\bar{b}h$ and $Zh$. There are several fake backgrounds contaminating this channel, *viz.* $c\bar{c}\gamma\gamma$, $jj\gamma\gamma$, $b\bar{b}jj$, $b\bar{b}j\gamma$ and $c\bar{c}j\gamma$. We estimate the yield from $c\bar{c}\gamma\gamma$ and $jj\gamma\gamma$ backgrounds by scaling: $N^{c\bar{c}\gamma\gamma\ (jj\gamma\gamma)} = (N^{c\bar{c}\gamma\gamma\ (jj\gamma\gamma)}_{\rm ATLAS}/N^{b\bar{b}\gamma\gamma}_{\rm ATLAS}) \cdot N^{b\bar{b}\gamma\gamma}$, where the numbers of $N_{\rm ATLAS}$ are taken from [17], whereas $N^{b\bar{b}\gamma\gamma}$ is our simulated number. Similarly, $c\bar{c}j\gamma$ is scaled as $N^{c\bar{c}j\gamma} = (N^{c\bar{c}j\gamma}_{\rm ATLAS}/N^{b\bar{b}j\gamma}_{\rm ATLAS}) \cdot N^{b\bar{b}j\gamma}$. Next, we select events containing exactly two $b$-tagged jets and two photons in the final state satisfying $p_{T,b_1(b_2)} > 40$ (30) GeV with $|\eta_{b_1,b_2}| < 2.4$ and $p_{T,\gamma} > 30$ GeV with $|\eta_\gamma| < 1.37$ (barrel) or $1.52 < |\eta_\gamma| < 2.37$ (endcap) respectively. Events are vetoed having leptons with $p_T > 25$ GeV and $|\eta| < 2.5$. After that, we do a cut-based analysis with the following selection cuts in sequence. Events must have $< 6$ jets to reduce the $t\bar{t}h$ background. The distance between two objects in the $\eta - \phi$ plane is defined as, $\Delta R = \sqrt{(}\Delta\eta^2 + \Delta\phi^2)$ where $\Delta\eta$ is the separation in the pseudorapidity plane and $\Delta\phi$ is the azimuthal angle separation between them. The $\Delta R$ between photons and b-jets are required to be within $\Delta R_{bb,\gamma\gamma,b\gamma} = [0.4 : 2.0]$. The invariant mass of b-jet pair and two photons must satisfy 100 GeV $< m_{bb} <$ 150 GeV and 122 GeV $< m_{\gamma\gamma} <$ 128 GeV respectively. Finally we put cuts on the transverse momentum of the Higgs boson constructed from the two b-jets and photons, $p_{T,bb/\gamma\gamma} > 80$ GeV. We got a signal significance of $S/\sqrt{B} = 1.46$ where S and B refers to the signal and total background yield respectively. Next we perform a multivariate analysis using BDT algorithm with the following kinematic variables:

$$m_{bb}, p_{T,\gamma\gamma}, \Delta R_{\gamma\gamma}, p_{T,bb}, \Delta R_{b_1\gamma_1}, p_{T,\gamma_1}, \Delta R_{bb}, p_{T,\gamma_2}, \Delta R_{b_2\gamma_1}, \Delta R_{b_2\gamma_2}, p_{T,b_1}, \Delta R_{b_1\gamma_2}, p_{T,b_2}, \not{E}_T$$

where all the objects are $p_T$ ordered. The signal significance is improved almost 20% ($S/\sqrt{B} = 1.76$) over the cut-based analysis.

*2.2. The $b\bar{b}\tau\tau$ channel*

The production rate in this $b\bar{b}\tau\tau$ channel is large as compared to the previous one. We divide this channel according to whether the $\tau$ leptons decay leptonically ($\tau_\ell$) and/or hadronically ($\tau_h$), *viz.* $b\bar{b}\tau_h\tau_h$, $b\bar{b}\tau_h\tau_\ell$ and $b\bar{b}\tau_\ell\tau_\ell$. $t\bar{t}$ production constitutes the dominant background in this channel which we generate in fully hadronic, semi-leptonic and fully leptonic final states. We also generate the sub-dominant backgrounds, *viz.* $b\bar{b}h$, $Zh$, $t\bar{t}W$, $t\bar{t}Z$, $t\bar{t}h$ and $b\bar{b}jj$ where jets can fake as hadronic $\tau$ jets. In this study, a different isolation criteria is used for the leptons following [18], where leptons are isolated if the energy activity within $\Delta R = 0.2$ around the lepton is less than 10 GeV. The $\tau$ jets satisfying $p_T > 20$ GeV and $|\eta| < 2.3$, are selected with tagging efficiencies of 55% and 50% along with $j \to \tau$ fake rates of 5% and 2% respectively for the one-pronged and three-pronged $\tau$'s [19]. Events must contain two $b$-tagged jets with $p_{T,b_1(b_2)} = 40$ (30) GeV and $|\eta| < 2.5$ and two $\tau$ objects. Also, we put some common cuts in all the three channels, *viz.* $m_{bb} > 50$, $\Delta R_{b\tau} > 0.4$, $\Delta R_{\tau\tau} > 0.4$, $m_{\tau\tau}^{\rm vis} > 30$ GeV (*vis* refers to the visible objects from $\tau$ decay products), $0.4 < \Delta R_{bb} < 2.0$ and 100 GeV $< m_{bb} <$ 150 GeV. After that, we do a cut based analysis by optimising over the following variables, $p_{T,bb}$, stransverse mass ($m_{T2}$) and visible $\tau\tau$ invariant mass ($m_{\tau\tau}^{\rm vis}$) or collinear mass ($M_{\tau\tau}$). We also perform BDT analysis in all the 3 final states. The fully hadronic channel among them, i.e. $b\bar{b}\tau_h\tau_h$ gives the highest signal significance.

*2.3. The $b\bar{b}WW^*$ channel*

The analysis in this channel is performed in two different search channels *viz.*, the fully leptonic ($b\bar{b}\ell\ell + \not{E}_T$) and the semi-leptonic ($b\bar{b}\ell + \text{jets} + \not{E}_T$) where $\ell$ denotes an electron, muon or a tau lepton. The dominant background contribution comes from $t\bar{t}$, among which only the $t\bar{t}$ leptonic contributes to the fully leptonic channel. In the semi-leptonic channel, the next dominant background arises from $Wb\bar{b}+$jets. We also simulate other sub-dominant backgrounds, *viz.* $b\bar{b}h$, $t\bar{t}h$, $t\bar{t}Z$, $t\bar{t}W$ and $\ell\ell b\bar{b}$. After applying the basic trigger cuts we do BDT analysis in the fully leptonic channel with variables:

$$p_{T,\ell_{1/2}},\ \not{E}_T,\ m_{\ell\ell},\ m_{bb},\ \Delta R_{\ell\ell},\ \Delta R_{bb},\ p_{T,bb},\ p_{T,\ell\ell},\ \Delta\phi_{bb\,\ell\ell},$$

and obtain a signal significance of $\sim 0.62$. In case of semi-leptonic channel we use these variables,

$$p_{T,\ell},\ \not{E}_T,\ m_{jj},\ m_{bb},\ \Delta R_{jj},\ \Delta R_{bb},\ p_{T,bb},\ p_{T,\ell jj},\ \Delta\phi_{bb\,\ell jj},\ \Delta R_{\ell\,jj},$$

for the BDT analysis which results in a signal significance of $\sim 0.13$.

*2.4. The $\gamma\gamma WW^*$ channel*

This channel is clean in terms of the photons in the final state and also the leptonic final states depending on the decay products of $W$ bosons. In case of fully leptonic channel, the backgrounds consist of $t\bar{t}h$, $Zh+$ jets and $\ell\ell\gamma\gamma+$ jets. Here, we select two isolated photons and leptons, where invariant mass of photons satisfies, 122 GeV $< m_{\gamma\gamma} <$ 128 GeV. We utilise the following variables to do the BDT analysis,

$$p_{T,\ell_{(1,2)}},\ \not{E}_T,\ m_{\ell\ell},\ m_{\gamma\gamma},\ \Delta R_{\gamma\gamma(\ell\ell)},\ p_{T,\ell\ell},\ p_{T,\gamma\gamma},\ \Delta\phi_{\ell\ell\,\gamma\gamma}.$$

After the BDT analysis, we observe a large improvement in the $S/B$ ratio from $4.4\times10^{-3}$ to 0.40. This channel can be important at higher energy collider. For the semi-leptonic channel, additional backgrounds arise, *viz.* $Wh$ + jets and $\ell\nu\gamma\gamma$ + jets. We get the $S/B$ ratio of 0.11 after performing a BDT analysis with the following variables:

$$p_{T,\ell_1},\ \not{E}_T,\ m_{\gamma\gamma},\ \Delta R_{\gamma\gamma},\ \ p_{T,\gamma\gamma},\ p_{T,\ell j},\ \Delta\phi_{\ell j\,\gamma\gamma},\ \Delta R_{\ell j},\ m_T.$$

*2.5. The 4W channel*

Finally, we analyse the $4W$ final state on which no previous study is performed. We divide this channel into 3 categories depending on the decay products from $W$ bosons, viz. same-sign di-lepton channel ($SS2\ell$): $\ell^{\pm}\ell^{\pm}+4j+\not{E}_T$, tri-leptons channel ($3\ell$): $3\ell+2j+\not{E}_T$ and four leptons channel ($4\ell$): $4\ell+\not{E}_T$. We train our BDT algorithm to separate signal and backgrounds. In $SS2\ell$ channel, we get a signal significance of 0.11 with $S/B \sim 10^{-3}$. So, this channel does not have much hope even at the HL-LHC. For the $3\ell$ final state, the signal significance improves slightly over the $SS2\ell$ channel, yielding $S/\sqrt{B} = 0.2$. However, we could not perform a multivariate analysis in the $4\ell$ channel owing to very small signal events with increased number of leptons in the final state.

*2.6. Modifying the Higgs self-coupling*

In this part, we analyse di-Higgs production upon varying the Higgs self-coupling from its SM value, defined as $\kappa = \lambda_{hhh}/\lambda_{SM}$. We choose 5 possible values of $\kappa$, *viz.* $-1$, 1, 2, 5 and 7. We perform four kind of analysis: standard cut-based analysis optimised for $\kappa = 1$, BDT analysis optimised for $\kappa = 1$ and $\kappa = 5$, and BDT analysis optimised for each signal cases. After doing the analysis, we obtain the following ranges of $\kappa$ values by employing the log-likelihood confidence level (CL) hypothesis test [23]:

$-0.86 < \kappa < 7.96$ CBA for $\kappa = 1$ optimisation; SM null hypothesis
$-0.63 < \kappa < 8.07$ BDT analysis for $\kappa = 1$ optimisation; SM null hypothesis
$-0.81 < \kappa < 6.06$ BDT analysis for $\kappa = 5$ optimisation; SM null hypothesis
$-1.24 < \kappa < 6.49$ BDT analysis for $\kappa = 5$ optimisation; $\kappa = 5$ null hypothesis.

In figure 1, we show the variation of $p_{T,\gamma\gamma}$ distribution with different Higgs self-coupling values.

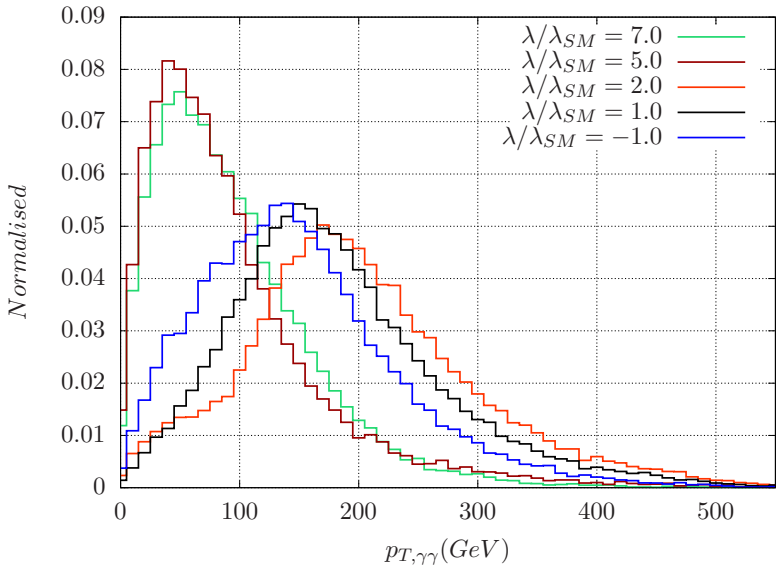


**Figure 1.** Normalised distributions of $p_{T,\gamma\gamma}$ for the signal with different $\lambda_{hhh}/\lambda_{SM}$ values after the basic selection cuts.

*2.7. Contamination from new physics processes*
We saw that di-Higgs production rate is very small and hence a small number of events is expected at the experiment. This small number can easily get contaminated by various beyond the SM (BSM) physics. If we perform a multivariate analysis to maximise the SM di-Higgs signal yield, there are two possible ways by which new physics can contaminate the search. Either the new physics scenario has overlapping kinematic distributions or the production rate is larger compared to SM di-Higgs production when the overlap is not significant. Here, we divide our analysis into 3 parts, *viz.* Double Higgs production, $pp \to hh(+X)$ through resonant or non-resonant production modes, single Higgs production in association with some other particles, $pp \to h + X$ and null Higgs scenario, $pp \to X$, yielding some of the final states as has been discussed in the earlier sections.

## 3. Higgs pair production at the HE-LHC

From the previous section we observe that the prospect of observing di-Higgs production at the HL-LHC is bleak. To obtain a better prospect, here we move on to proposed high energy collider at $\sqrt{s} = 27$ TeV with 15 $ab^{-1}$ of integrated luminosity and analyse various di-Higgs channels. The di-Higgs signal and backgrounds samples are generated by using `MG5_aMC@NLO` [11] with `NNPDF2.3LO` PDF set [20]. For showering and hadronisation, we use `Pythia8` [13]. The jets are reconstructed using anti-$kT$ [14] algorithm with jet radius parameter of $R = 0.4$ in the `FastJet` [15] framework. The detector effects are simulated using `Delphes-3.4.1` [16]. In this work, we perform three types of multivariate analysis, *viz.* the BDT algorithm, XGBoost toolkit, and DNN. Following [21], we fix the b-tagging efficiency, $c \to b$ and $j \to b$ mistagging efficiency. We use the following modified signal significance formula [22]:

$$\mathcal{S} = \sqrt{2\left((S+B)\log\left(1+\frac{S}{B}\right) - S\right)},$$

where $S$ and $B$ refer to the signal and total background yield after doing the multivariate analyses.

*3.1. The $b\bar{b}\gamma\gamma$ channel*
We select exactly two b-jets and photons in the final state and apply similar trigger cuts as before in section 2.1. We choose the following 19 kinematic variables and perform multivariate analysis using the BDT algorithm, the XGBoost toolkit, and DNN:

$$m_{bb},\ \Delta R_{\gamma\gamma},\ \Delta R_{bb},\ p_{T,bb},\ p_{T,\gamma\gamma},\ \Delta R_{bb\,\gamma\gamma},\ p_{T,hh},\ \Delta R_{b_i\gamma_i},$$
$$m_{hh},\ p_{T,b_{1,2}},\ p_{T,\gamma_{1,2}},\ \not{E}_T,\ \cos\theta^*,\ \cos\theta_{\gamma_1 h}.$$

The $\cos\theta^*$ variable is defined as:

$$\cos\theta^* = \frac{Sinh(\eta_{\gamma 1} - \eta_{\gamma 2})}{\sqrt{1 + (p_{T,\gamma\gamma}/m_{\gamma\gamma})^2}}\ \frac{2\ p_{T,\gamma 1}\ p_{T,\gamma 2}}{m^2_{\gamma\gamma}}.$$

The $\theta_{\gamma_1 h}$ represents the angle between the hardest photon direction in the Higgs rest frame and the Higgs boson direction in the lab frame. The XGBoost analysis performs better than the BDT and DNN analysis and we got a signal significance of 12.46, 9.42 and 10.03 respectively. Since the choice of probability cut applied on the XGBoost result is subjective and can give rise to different results with different choices, we show the variation of signal significance with probability cut in figure 2.

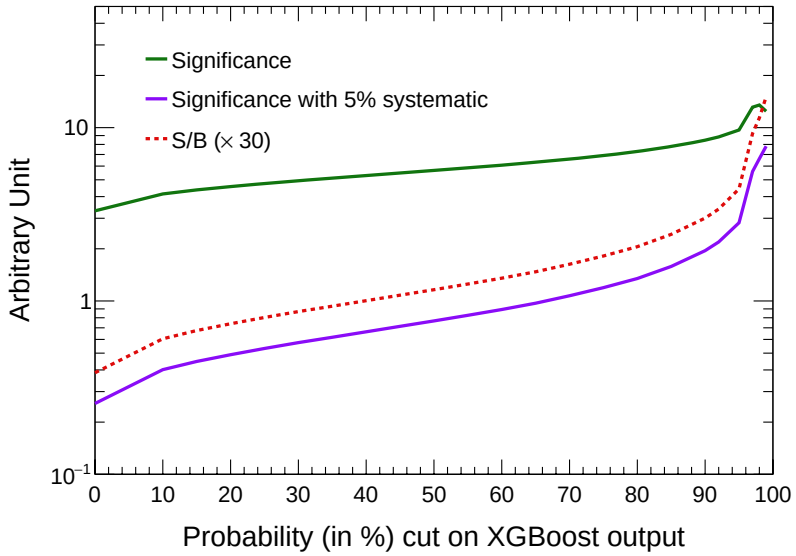


**Figure 2.** *The variation of significance (with (5%) and without systematic uncertainty) and $S/B$ is shown as a function of the probability cut on the XGBoost output for the $b\bar{b}\gamma\gamma$ channel.*

*3.2. The $b\bar{b}\tau\tau$ channel*

Here, we analyse the channel with fully hadronic decay of the $\tau$'s because we observe that this channel is the most sensitive channel in our previous HL-LHC study. Events are selected with exactly two $b$-tagged jets and $\tau$-tagged jets in the final state. After putting basic cuts we do the multivariate analysis with the following variables:

$$p_{T,bb},\ \Delta R_{bb},\ m_{bb},\ p_{T,\tau_h\tau_h},\ \Delta R_{\tau_h\tau_h},\ \Delta\phi_{\tau_{h1}\not{E}_T},\ \Delta\phi_{\tau_{h2}\not{E}_T},$$
$$m_{T,\tau_h\tau_h},\ m^{col}_{\tau_h\tau_h},\ m_{T2},\ m_{\rm eff},\ \Delta R_{b_1\tau_{h1}},\ p^{\rm vis}_{T,hh},\ m^{\rm vis}_{hh},\ \Delta R^{\rm vis}_{hh}.$$

We obtain a signal significance of 2.77, 4.78 and 4.25 from BDT, XGBoost and DNN analyses respectively.

*3.3. The $b\bar{b}WW^*$ channel*

Over the 3 possible final states, we choose the cleanest fully leptonic channel from $b\bar{b}WW^*$. We demand exactly two isolated leptons and $b$-jets in the final state. Several kinematic variables are chosen for the multivariate analysis:

$$logT,\ logH,\ M^{(b)}_{T2},\ M^{(\ell)}_{T2},\ \sqrt{\hat{s}^{(\ell\ell)}_{min}},\ \sqrt{\hat{s}^{(bb\ell\ell)}_{min}},\ p_{T,\ell_{1/2}},\ \not{E}_T,\ m_{\ell\ell},\ m_{bb},$$
$$\Delta R_{\ell\ell},\ \Delta R_{bb},\ p_{T,bb},\ p_{T,\ell\ell},\ \Delta\phi_{bb\,\ell\ell}.$$

The signal significance is higher in case of XGBoost analysis, $\sim 2.75$ without any systematic uncertainty.

*3.4. The $WW^*\gamma\gamma$ channel*

Here, we select the fully leptonic final state from $W$ boson decay products. Since DNN analysis gives low performance compared to XGBoost, we only do the BDT and XGBoost analysis on

this channel and the following ones. Two isolated opposite sign leptons and two photons are selected and the following variables are chosen to do the multivariate analysis:

$$p_{T,\gamma\gamma},\ \Delta R_{\gamma\gamma},\ m_{\ell\ell},\ p_{T,\ell\ell},\ \Delta R_{\ell\ell},\ \Delta R_{\ell\ell\,\gamma\gamma},\ M_T,\ p_{T,hh},\ m_{eff},\ \Delta R_{\gamma_1\ell_1},\ Cos\theta^*,\ Cos\theta_{\gamma_1 h},\ \not{E}_T.$$

We obtain signal significance of 1.64 and 2.05 from BDT and XGBoost analysis respectively.

*3.5. The $b\bar{b}ZZ^*$ channel*

To study this channel, we dissect it into two leptonic final states, *viz.*

$$pp \to hh \to b\bar{b}ZZ^* \to b\bar{b}\ 4l',\ l' = e^{\pm}\ or\ \mu^{\pm}$$

$$pp \to hh \to b\bar{b}ZZ^* \to b\bar{b}\ e^+e^-\mu^+\mu^-$$

which makes the analysis easier when constructing kinematic variables. In case of $2b4l'$ channel, events are selected having exactly two $b$-jets and four isolated leptons in the final state satisfying 120 GeV $< m_{4l'} <$ 130 GeV. The following variables are used in the multivariate analysis:

$$p_{T,bb},\ \Delta R_{bb},\ m_{bb},\ p_{T,4\ell},\ m^{1,2}_{Z_i},\ \Delta R^{1,2}_{ZZ},\ m_{T2},\ m_{\text{eff}},\ \Delta R_{b_1\ell_1},\ m_{hh},\ \Delta R_{hh},\ \not{E}_T.$$

Similarly in the $2b2e2\mu$ channel, we select events with exactly 2 $b$-tagged jets, two isolated electrons and two isolated muons. The BDT and XGBoost analysis is performed using these following 13 variables:

$$p_{T,bb},\ \Delta R_{bb},\ m_{bb},\ p_{T,2e2\mu},\ m_{Z_i},\ \Delta R_{ZZ},\ m_{T2},\ m_{\text{eff}},\ \Delta R_{b_1\ell_1},\ m_{hh},\ \Delta R_{hh},\ \not{E}_T.$$

We get a combined signal significance of 1.3 from XGBoost analysis on these two final states.

*3.6. The $b\bar{b}\mu\mu$ channel*

The signal rate in this channel is lower than the $b\bar{b}\gamma\gamma$ channel because of the small $h \to \mu\mu$ branching ratio. This channel suffers from the huge $t\bar{t}$ and QCD-QED $b\bar{b}\mu\mu$ backgrounds. After selecting two $b$-jets and two muons in the final state, we put basic generation level cuts and perform the multivariate analysis with the following kinematic variables:

$$p_{T,\mu\mu},\ \Delta R_{\mu\mu},\ m_{\mu\mu},\ p_{T,bb},\ \Delta R_{bb},\ m_{bb},\ H_T,\ p_{T,hh},\ m_{hh},\ \Delta R_{hh},\ \not{E}_T.$$

To improve this analysis, one has to find better ways to reduce the $t\bar{t}$ and QCD-QED $b\bar{b}\mu\mu$ backgrounds.

## 4. Conclusion

In this work, we study the prospect of observing Higgs pair production through various final states. At the HL-LHC detector configuration, we perform cut-based as well as more sophisticated multivariate analysis to optimise signal over the background events. The $b\bar{b}\gamma\gamma$ channel is the most promising search channel to look for di-Higgs production which gives rise to signal significance of 1.76 from BDT analysis. Overall, we get a signal significance of $\sim 2.1$ after combining all the search channels considered here in case of HL-LHC analysis. Also, we study the effects on the analysis upon changing the Higgs self-coupling and we put limits on $\kappa$. One must be careful while searching for di-Higgs production as new physics can easily contaminate the small signal yield. Next, we search for di-Higgs prospects at HE-LHC detector configuration. Here, the di-Higgs production cross-section improves by a factor of $\sim 4$. We perform analysis using several machine learning techniques, *viz.* BDT algorithm, XGBoost toolkit and DNN. The analysis on $b\bar{b}\gamma\gamma$ channel alone resulted in a signal significance $\sim 10$ and the performance in other search channels are also improved. We conclude that di-Higgs production can be probed with discovery potential at the proposed HE-LHC.

**Acknowledgments**
This work was supported in part by the CNRS LIA-THEP (Theoretical High Energy Physics) and the INFRE-HEPNET (IndoFrench Network on High Energy Physics) of CEFIPRA/IFCPAR (Indo-French Centre for the Promotion of Advanced Research). SB is supported by a Durham Junior Research Fellowship COFUNDed between Durham University and the European Union under grant agreement number 609412. The work of BB is supported by the Department of Science and Technology, Government of India, under the Grant Agreement number IFA13-PH-75 (INSPIRE Faculty Award).

## References

[1] Aad G *et al.* (ATLAS collaboration) 2012 *Phys. Lett.* B **716** 1–29
[2] Chatrchyan S *et al.* (CMS collaboration) 2012 *Phys. Lett.* B **716** 30–61
[3] URL `https://twiki.cern.ch/twiki/bin/view/LHCPhysics/LHCHXSWGHH`
[4] Adhikary A, Banerjee S, Barman R K, Bhattacherjee B and Niyogi S 2018 *J. High Energy Phys.* **07** 116
[5] Hoecker A *et al.* 2007 *Preprint* `0703039`
[6] Adhikary A, Barman R K and Bhattacherjee B *Preprint* `2006.11879`
[7] Chen T and Guestrin C 2016 *KDD '16: Proceedings of the 22nd ACM SIGKDD International Conference on Knowledge Discovery and Data Mining* (New York: Association for Computing Machinery)
[8] Goodfellow I , Bengio Y and Courville A 2016 *Deep Learning* (MIT Press)
[9] URL `https://www.tensorflow.org/`
[10] URL `https://keras.io/`
[11] Alwall J *et al.* 2014 *J. High Energy Phys.* **07** 079
[12] Ball R D *et al.* 2013 *Nucl. Phys.* B **867** 244–289
[13] Sjostrand T *et al.* 2015 *Comput. Phys. Commun.* **191** 159–177
[14] Cacciari M, Salam G P and Soyez G 2008 *J. High Energy Phys.* **04** 063
[15] Cacciari M, Salam G P and Soyez G 2012 *Eur. Phys. J.* C **72** 1896
[16] de Favereau J *et al.* (DELPHES 3 Collaboration) 2014 *J. High Energy Phys.* **02** 057
[17] ATLAS Collaboration *Preprint* `ATL-PHYS-PUB-2017-001`
[18] ATLAS Collaboration *Preprint* `ATL-PHYS-PUB-2015-046`
[19] ATLAS Collaboration *Preprint* `ATL-PHYS-PUB-2013-004`
[20] Ball R D *et al.* (NNPDF Collaboration) 2015 *J. High Energy Phys.* **04** 040
[21] Sirunyan A M *et al.* (CMS collaboration) 2018 *J. Instrum.* **13** P05011
[22] Cowan G, Cranmer K, Gross E and Vitells O 2011 *Eur. Phys. J.* C **71** 1554
[23] Junk T 1999 *Nucl. Instrum. Meth.* A **434** 435–443